Medical Engineering and Physics 73 (2019) 92–99

Contents lists available at ScienceDirect

Medical Engineering and Physics

journal homepage: www.elsevier.com/locate/medengphy

Technical note

Assessment of sub-epidermal moisture by direct measurement of tissue biocapacitance

Graham Ross[a,*], Amit Gefen[b]

[a] Bruin Biometrics LLC (BBI), 10877 Wilshire Blvd., Suite 1600, Los Angeles, CA 90024, USA
[b] Department of Biomedical Engineering, Faculty of Engineering, Tel Aviv University, Tel Aviv 6997801, Israel

ARTICLE INFO

Article history:
Received 16 February 2019
Revised 22 June 2019
Accepted 18 July 2019

Keywords:
SEM scanner
Pressure ulcer prevention
Pressure injury
Localized edema
Laboratory testing and modeling

ABSTRACT

The noninvasive SEM Scanner technology described herein assesses the fluid contents of human skin and subdermal tissues to a depth of several millimeters. The device makes a direct steady-state measurement of the capacitance of its sensor, which is affected by the equivalent dielectric constant of the material (i.e. the layered tissue structures) that is within the electric field between the sensor electrodes. Calculation of a "delta" value that compares measurements from several sites, some of which will be healthy tissue, compensates for systemic changes and provides a consistent measure of tissue health condition. We describe the hardware, software and rigorous laboratory testing and computational modeling of the principles of operation of the SEM Scanner, for the first time in the literature. These studies revealed a detection depth of approximately 4 mm for an electric potential of 0.3 V. The novel SEM Scanner provides the first useful technological means to assess the health status of tissues below the stratum corneum in patients who are at-risk for pressure injuries.

1. Introduction

A pressure ulcer or pressure injury (PI) is a localized injury to the skin and/or underlying tissue usually over a bony prominence, such as the sacrum or calcaneus (heel bone). Current understanding of PI development is that cell and tissue damage may begin under the skin, and there may be significant tissue damage before symptoms such as discoloration are visible on the skin surface. This damage is characterized by an increase in fluid contents of tissues at the site of the forming PI due to inflammatory response triggered by chemokines that increase vascular permeability, resulting in evolving edema [1–3].

The only FDA-approved device which detects early PI damage through detection of an evolving (initially invisible) edema is the Sub-Epidermal Moisture (SEM) Scanner (model 200, Bruin Biometrics (BBI) LLC, Los Angeles CA, USA). While there are several devices offered for use in the cosmetic industry to assess the efficacy of skin moisturizers, these devices make an impedance measurement by passing a high-frequency signal through the examined skin and then extracting the capacitance value from the phase-shift of the signal [4,5]. Attempts to compare this capacitance value to a threshold have proven fruitless. This technical note describes the inherently different, novel technological SEM Scanner approach for early identification of PIs, and the principles underlying the design of this new medical device.

2. Methods

The SEM Scanner measures the steady-state local tissue capacitance between two electrodes. The electric field that is created between the electrodes projects outward from the plane of the electrodes and, when the electrodes are placed on the skin of a patient, the field projects into the epidermis and dermis. Changes in the measured biocapacitance are related to changes in the equivalent dielectric constant (DC, also "k") of the fluid contents in tissues that is within the electric field. The biocapacitance measurement is then converted to a pre-defined SEM scale that is a dimensionless measure of the local internal fluid contents in the examined tissue region, through a linear unit-of-measure conversion. Inter-operator and inter-device reliability of the SEM Scanner exceeds 0.80 [6]. The principles of design of this new device and the measurement process are described in detail below.

Abbreviations: A, area; C, capacitance; CDC, capacitance-to-digital converter; d, distance; DC, dielectric constant, also referred to as "k"; ED, epidermis/dermis tissue layer; FEA, finite element analysis; FR4, a standard fiberglass substrate used in printed circuit boards; LiPo, lithium polymer; m, meter; N, newton; pF, picofarad; PI, pressure injury; SC, stratum corneum; SEM, sub-epidermal moisture; SPDT, single-pole double-throw; Q, coulomb; κ, dielectric constant; ε_0, permittivity of free space.

* Corresponding author.
E-mail address: gefen@tauex.tau.ac.il (A. Gefen).

https://doi.org/10.1016/j.medengphy.2019.07.011
1350-4533/

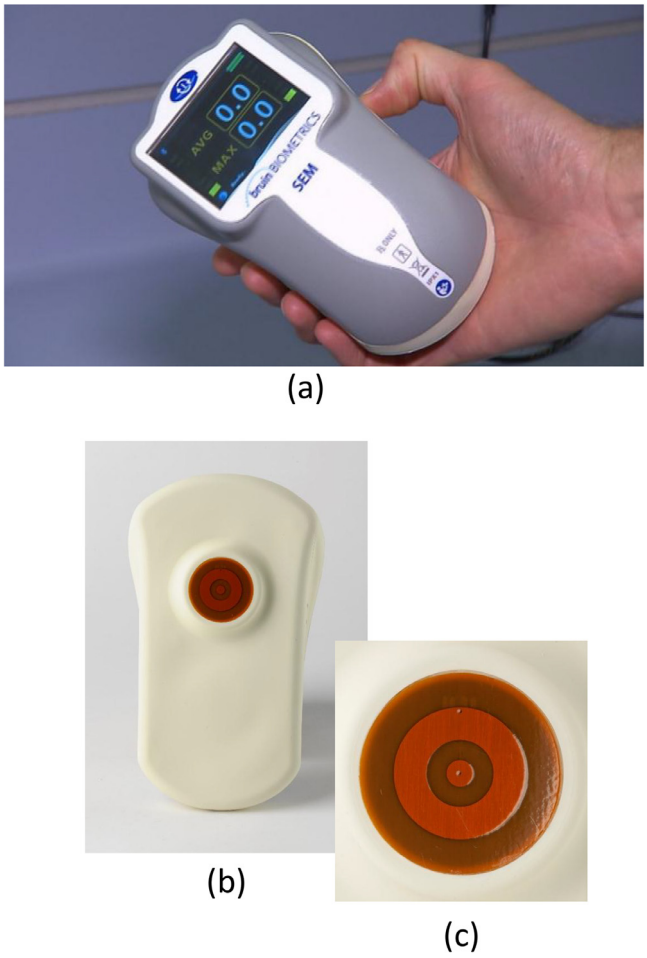

Figure 1. (a) The front of the self-contained, handheld subepidermal moisture (SEM) Scanner 200 model. (b) The back side of the Scanner, with enlarged detail view and (c) of the SEM sensor.

2.1. Hardware

The SEM Scanner is a self-contained handheld device (Fig. 1a) for detecting intra-tissue localized fluid content changes [7–10]. It incorporates a display screen on the front where SEM values and the intensity of force applied by a user to ensure adequate skin-device contact are presented. The sensor is located on a raised portion of the flexible back surface (Fig. 1b and c). The raised portion is spring-mounted with an internal force sensor. The biocapacitance measurement is affected by the skin-device contact force [11], and hence, a force sensor has been included to minimize variability across users [6] as applying largely varying amounts of force may push different fluid contents away from the device-skin contact site. When the user presses the sensor against the skin of a patient, the spring under the sensor is compressed and the applied force is displayed in a bar-graph. When the applied force is within a target range of 3.9–5.9 N, a SEM measurement is automatically taken.[1] When the applied force is removed (as when the user removes the SEM Scanner from the skin) the device resets and is ready to take another measurement.

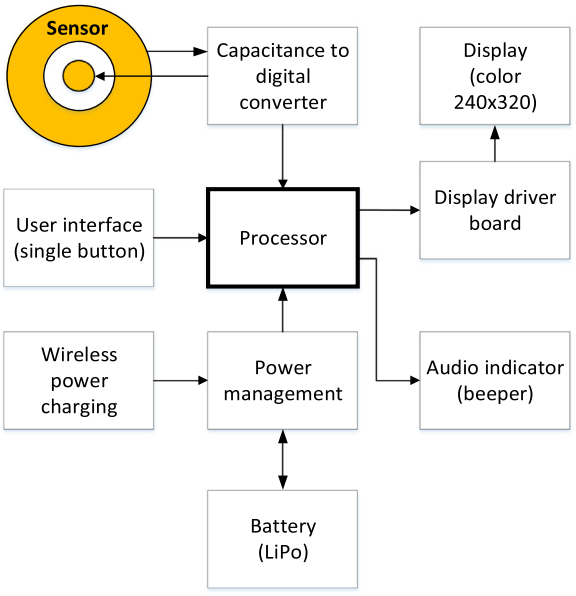

Figure 2. The (a) hardware block diagram and (b) the components that handle the data flow of a capacitance measurement. The processor is an Atmel ATMEGA644P-20AU. The program code is written in C with the use of standard pre-compiled libraries.

The sensor itself is a coplanar, concentric capacitor with a round electrode (diameter= 4 mm) surrounded by a toroidal electrode (with outer and inner diameters of 20 mm and 10 mm, respectively) which are formed by copper plating (Fig. 1c). The electrode surfaces are isolated by a thin layer of polyimide and are shielded from the internal electronics. The two electrodes are directly and individually connected to a capacitance-to-digital converter (CDC) that is connected to a processor (Fig. 2). The CDC is continuously measuring the capacitance between the two electrodes and converts the recorded measurement to a SEM value shown on the display when the applied force is within the above target range.

2.2. Software

The SEM Scanner utilizes a purpose-built chip (Analog Devices, Norwood, MA, USA) to directly measure the biocapacitance of soft tissues between the sensor electrodes using a sigma-delta conversion process [12,13]. This measurement of biocapacitance (in picofarads) is converted by this processor to a non-dimensional scale of SEM values. The SEM Scanner compares the SEM values from a set of measurements taken in close proximity at a certain body location to calculate a "delta" value that is the parameter of clinical interest, as described below.

2.2.1. Sigma-delta measurements of the biocapacitance

The sigma-delta architecture of the CDC is shown in Figure 3a. The CDC includes an internal reference capacitor (C_{REF}) having one electrode that can be connected to either a positive internal reference voltage ($+V_{REF}$) or a negative internal reference voltage ($-V_{REF}$) through a single-pole double-throw (SPDT) switch S1. The other electrode of C_{REF} can be connected to either the summing input of an integrator (OP1) or ground through SPDT switch S2.

The sensor of the SEM Scanner is treated as a variable capacitor of unknown capacitance. One electrode of the capacitor is connected to an excitation signal generated by the CDC. The other electrode of the sensor is connected through a SPDT switch S3 to

[1] Performing valid SEM measurements requires training and practice. A trained operator can identify a wrong SEM measurement from a set of such measurements as the wrong SEM value will be considerably different from other readings of that anatomical area. Inclusion of a wrong SEM measurement in a delta calculation may generate a "false positive" delta value, which may then lead a clinician to implement preventive interventions that would have no harmful effects on the examined patient.

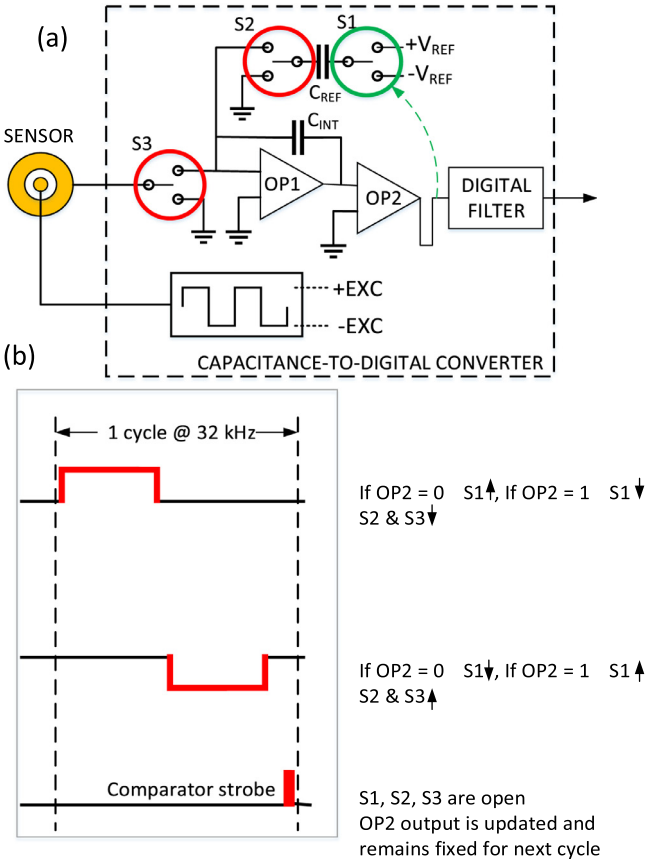

Figure 3. During the positive phase of the "excitation," the switches are configured as shown below, (a) wherein when the comparator output is "0," the reference capacitor is charged by $V+$, (b) and when the comparator output is "1," the reference capacitor is charged by $V-$, (c) during the negative phase of the "excitation," the switches are reversed as shown to connect the charged sensor and the charged reference capacitor to the CINT capacitor, (d) the nominal "excitation" is really a patterned activation of switches that connect the sensor and the reference capacitor to one of the $V+$ or $V-$ sources. At the end of each "square wave," the comparator is pulsed and the output may change based on the summed charge on the CINT capacitor (the input to the op amp).

either the summing input of OP1 or to ground. The excitation signal switches between a +EXC voltage and a −EXC voltage.

All of the switches S1, S2, S3 switch back and forth between the two poles with brief periods of "no connect" between each connection. The polarity of the connection of switch S1 is determined by the output state of the comparator OP2 during the previous cycle. If the output is a "1," this indicates that there is a net positive charge remaining on the summing junction of integrator OP1 and $-V_{REF}$ will be used to charge C_{REF} by setting S1 to be "up" (Fig. 3a) during the charging phase of the cycle. If the output is a "0," this indicates that there is a net negative charge remaining on the summing junction of OP1 and $+V_{REF}$ will be used to charge C_{REF} by setting S1 to be "down" during the charging phase of the cycle.

The time constants of the circuit elements are low enough that the voltages on each connected segment of the circuit reaches equilibrium long before the end of each phase. The sensor is charged up to a steady-state voltage, either +EXC or −EXC, during each phase although the amount of charge Q required to achieve that voltage is dependent upon the biocapacitance during the respective phase. Even though the excitation pulses are provided at a rate of 32,000 pulses per second, each phase of each pulse is a steady-state measurement of the biocapacitance at that instant.

After both the positive and negative phases of a pulse are complete, and while all the switches are not connected so that the voltage on the summing junction of OP1 is constant, the comparator OP2 is "strobed" and the output will now reflect the new voltage on the summing junction. This output will remain constant until the strobe of the next pulse.

2.2.2. Conversion to SEM units

The measured biocapacitance, in picofarads, is sent digitally from the CDC to the processor. For clinical utility, the processor converts the measured biocapacitance to a dimensionless "SEM value" using a linear "$ax+b$" conversion algorithm, where the parameters "a" and "b" are determined for each unit at the time of manufacture. Calibration measurements are made with the sensor exposed to open air and with the sensor in contact with pure water, which bound the range of moisture content of tissue.[2] The SEM value is then shown on the display (Fig. 1a) and stored internally. The processor has 64 kB of non-volatile memory. The device stores only the most recent set of SEM values associated with a single body location of a single patient. This is normally a maximum of six measurements. The device is reset between each body location. SEM values range from approximately 0.3 for a measurement taken in open air (which corresponds to a dielectric constant of ∼1) to approximately 3.9 for a measurement with the sensor submerged in pure water (dielectric constant of ∼80).

2.2.3. Calculation of "delta" value

The parameter of primary clinical interest is the difference in the SEM values between healthy tissue and an adjacent tissue region that may have subsurface damage which affected local tissue fluid contents (i.e. the inflammatory response has triggered micro-scale edema). For example, a set of 4–6 measurements may be taken in a small area of the body wherein tissues have a similar structure, e.g. the left versus right body sides near the sacrum. Since the SEM Scanner primarily targets micro scale edema as a result of the inflammatory response, then even if such localized damage already occurred, it is almost certain that at least one of the measurements across the different (nearby) locations will be over healthy (non-damaged) tissue. The SEM Scanner compares the set of acquired SEM values to each other and calculates the delta value as the difference between the highest and lowest values in the set. A healthy patient will have a fairly uniform set of SEM values acquired from an anatomical site (as all measurement points will reflect normal tissue), resulting in a low (typically 0.0–0.2) delta value for that area [1–3,6]. Larger delta values are an indication that there is an increased risk of tissue damage in at least one point of the examined area, reflected in non-uniform tissue fluid contents due to the localized build-up of edema.

2.3. Laboratory testing and modeling of the principles of operation of the SEM Scanner

2.3.1. Bench test configuration

Laboratory experiments were conducted to verify that the SEM values displayed by the SEM Scanner change in proportion to the amount of water within the electric field of the sensor. Tests in bulk fluid media were chosen so that a single low-dielectric

[2] Each device is calibrated at the end of the production line. There is a calibration subroutine in the embedded code within the internal processor that is accessed through non-standard manipulation of the device. Using a special fixture, the workflow of the calibration subroutine has the operator make a first measurement with the sensor electrodes exposed to open air and a second measurement with the sensor electrodes in contact with pure water. The subroutine considers the measurements as "x" values and the SEM values (0.3, 0.9) that are defined in the embedded code as "y" values. With two sets of "x" and "y" values, the subroutine calculates the "a" and "b" parameters and stores them in non-volatile memory, and then exits the calibration process.

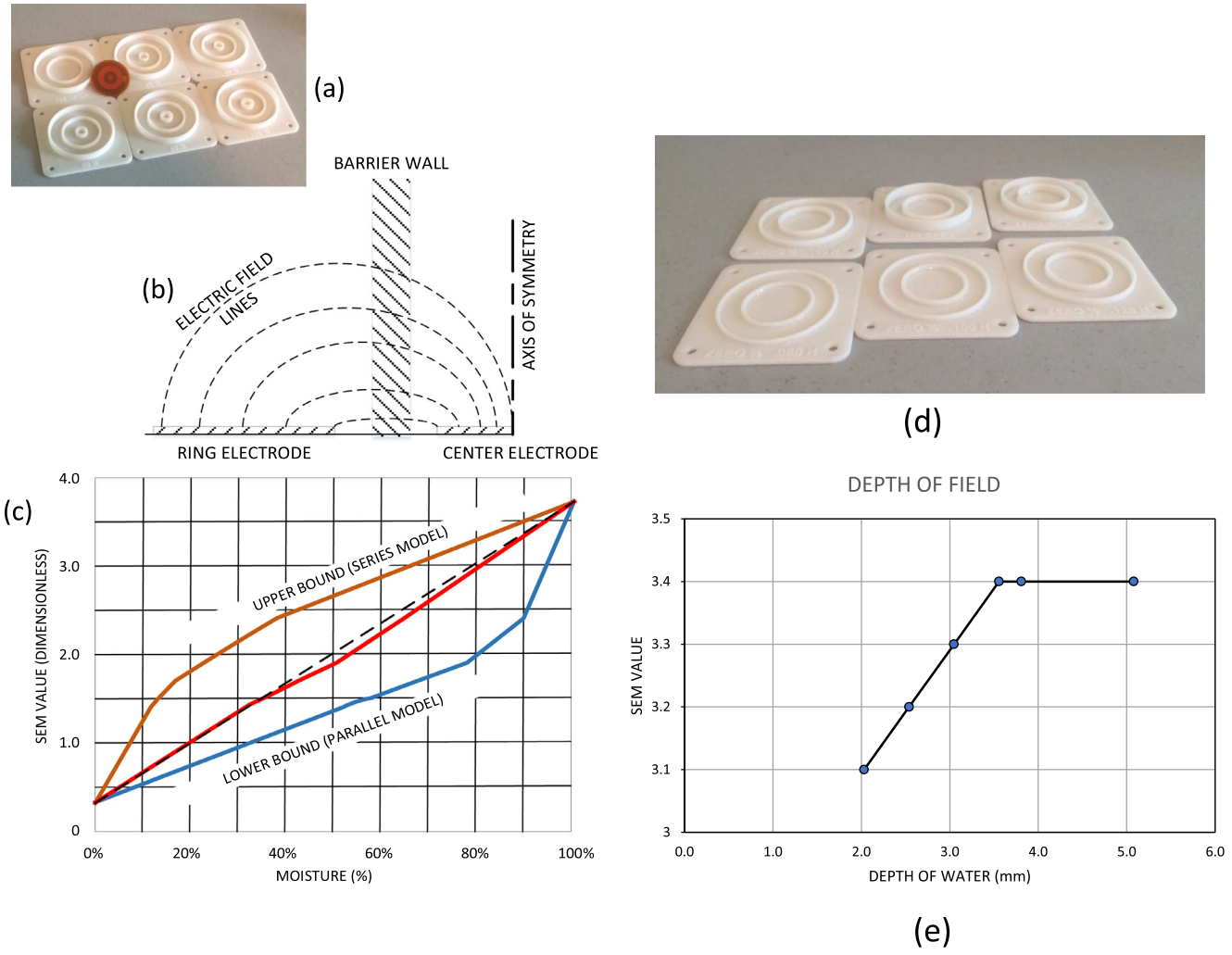

Figure 4. Experimental characterization of the SEM Scanner technology: picture (a) depicts the set of fixtures used to measure the SEM value for various moisture contents, which are varied by the thickness of the innermost wall of the fixture. Diagram (b) shows how the field lines that connect the two electrodes of the sensor pass through the barrier wall. The first chart (c) plots the SEM values provided by the SEM Scanner 200 against a calculated water percentage. The orange and blue lines indicate the upper and lower bounds of a mixed-dielectric model and the red line is an average of these bounds, while the black dashed line is a linear connection of the end points, provided as a reference. Picture (d) depicts the set of fixtures used to measure the SEM value for various depths of water, which are varied by the height of the walls of each fixture. The second chart (e) plots the SEM values provided the SEM Scanner 200 when used to test trays having various depths of water, wherein the Scanner does not respond to additional water further than from the sensor.

Table 1
Barrier wall thicknesses of fixtures.

Fixture no.	Fluid fraction (%)	Barrier wall thickness (mm)	Diameter of well wall (mm)	Diameter of containment wall (mm)
1	100	0	25	45
2	91	0.64		
3	81	1.53		
4	72	1.93		
5	63	2.54		
6	57	3.10		

element could be introduced to displace a known amount of high-dielectric water and provide a known water fraction within the electric field of the sensor. The test fixtures, shown in Figure 4a, were three-dimensionally printed with pools of water of sufficient depth to meet or exceed the previously estimated penetration depth (3.8 mm) of the sensor field. The fixtures had a circular plastic wall that extended the full depth of the pool and touched the sensor in the gap between the two electrodes, thus ensuring that all the field lines between the two electrodes would pass through the plastic wall (Fig. 4b). The amount of water within the electric field was inversely related to the thickness of the wall, as all other geometric features were constant. The walls of the fixtures each had a different thickness, as listed in Table 1, including a fixture with no wall. The maximum wall thickness was set equal to the gap between the electrodes, as any overlap of the wall and either electrode would allow some part of the field to bypass the full thickness. The lesser thicknesses were chosen to provide four intermediate thicknesses between the maximum thickness and zero (no wall) (Table 1).

Additional experiments were run to verify that the depth of the electric field is sensitive to differences in DCs. Test fixtures that were similar in design to the first set of fixtures, but with variable depths of the pool of water (as listed in Table 2) and no circular wall, were 3D printed for this purpose. These fixtures are shown

Table 2
Depth of water within fixtures.

Fixture no.	Well wall height (mm)	Diameter of well wall (mm)	Height of containment wall (mm)	Diameter of containment wall (mm)
1	5.08	25	5.08	45
2	3.81		3.81	
3	3.56		3.56	
4	3.05		3.05	
5	2.54		2.54	
6	2.03		2.03	

Table 3
Characteristics of the model components.

Material	Dielectric constant	Thickness (mm)	Inner diameter (mm)	Outer diameter (mm)
Ground plane	–	–	0	28.58
FR4	4.7	0.41	0	31.75
Inner electrode	–	0.04	0	4.32
Outer electrode	–	0.04	10.16	20.32
Adhesive	3.6	0.03	0	31.75
Polyimide	3.6	0.03	0	31.75
Stratum corneum	16	0.01	0	31.75
Epidermis/dermis	60	25.44	0	31.75

in Figure 4d. If the electric field penetrated deeper than the depth of water in the pool of a fixture, the field would penetrate into the plastic of the fixture (and potentially deeper into the table). As the DC of plastic is ~20× lower than water, the SEM value reported for a fixture with a shallow pool of water would be lower than that reported for a fixture with a deeper pool of water.

2.3.2. Computational modeling

A computational finite element (FE) model was developed for analyzing the static electric field of the sensor, particularly for understanding the field shape and electric potential distribution including the depth of field penetration into tissues which is not predictable analytically [7]. A second purpose was to predict the total biocapacitance of simulated tissues within the electric field. We assumed full contact between the sensor and skin but no tissue deformations resulting from that contact. Under these conditions, the FE model was used to evaluate the ability of the sensor to detect a change from a healthy tissue condition (modeled as 70% water) [8–11,14] to fully-developed edema (i.e. pure water) at various tissue depths. If the transition to fully-developed edema was deeper than the sensitive depth of the electric field, then the effective biocapacitance would not be affected. As the simulated transition to edema is moved closer to the skin surface and the sensor, the biocapacitance will increase in proportion to how much of the water is within the field. The governing equations for the electric field are the Maxwell equations.

As the sensor is axisymmetric and assumed to be held in a perfectly horizontal orientation on the skin, a 2D model of a plane passing through the center of the sensor was considered sufficient to analyze the field. The skin was represented as a surface stratum corneum (SC) layer covering epidermis/dermis (ED) tissue, both with uniform thicknesses and isotropic electrical properties. The overall thickness of the model was chosen so that it far exceeded any possible depth of the field.

The boundary conditions are 1.8 V applied to the nodes of the surface of the center electrode and 0 V applied to the nodes on the surfaces of the outer electrode and the ground plane. The primary unknowns (nodal degrees of freedom) that the FE solver calculates are electric scalar potentials, i.e. voltages.

For the baseline simulation case, the SC was modeled as 'dry' (with DC=16 approximating that of collagen [9]) and the ED was assumed to contain 70% water (DC=60) [8–11,14]. Dimensions and dielectric constants of all the model components are listed in Table 3. The copper electrodes and the ground plane were represented as boundary conditions on the geometry edges. Specifically, the center electrode was simulated to held at 1.8 V while the ground plane and outer electrode were held at 0 V.

The FE model was developed using the software ANSYS Mechanical v17.2 (Canonsburg, PA, USA). The model was constructed from PLANE121 elements, which are 2-D, 8-node, charge-based electric elements and are well suited to model curved boundaries and material transitions. This element has one degree of freedom (voltage) at each node and compatible voltage shapes. The mesh sensitivity of the modeling was evaluated using 3 different mesh densities with horizontal element widths of 0.0265, 0.0132 and 0.0079 mm. The element height was changed proportional to the change in the element width. These sensitivity analyses revealed that the modeling outcomes of field penetration depth and biocapacitance were not sensitive to element sizes below 0.0132 mm. Accordingly, an element size of 0.0079 mm was used to obtain the results reported here. The numerical procedure was validated by evaluating a parallel plate capacitor modeled as two circular parallel plates with 1 m radius, an area $(A)=\pi(1)^2=\pi\,m^2$, a distance (d) between the plates= 0.125 m, the space between the plates filled with air having a DC= 1 and a permittivity $(\varepsilon_0)=8.854$ pF/m (free space). With a 5 V difference across the plates, the theoretical value of the plate capacitance= $\kappa\varepsilon_0(A/d)$ =222.5 pF. The closed form solution provides a value of 222.5 pF as well, thus confirming the validity of our numerical modeling methodology.

3. Results

3.1. Bench test to establish correlation of SEM readings with water contents

The effective DC of a mixture of two materials cannot be precisely predicted by means of closed-form analytical modeling [7], and so an empirical approach supported by computational simulations is necessary. In the fixtures tested in our experimental work, a layer of low-dielectric material was created by the barrier wall that was positioned under the gap between the electrodes (Fig. 4a). The bulk of the electric field passes through high-dielectric water on both sides of the barrier wall, creating a 3-layer water-plastic-water layered mixture (Fig. 4b). The effective DC resulting from the plastic-water combination can be bounded between an experimental configuration consisting of multiple layers aligned with the field (a parallel element model) and a model consisting of multiple layers aligned perpendicular to the field (a series model). The

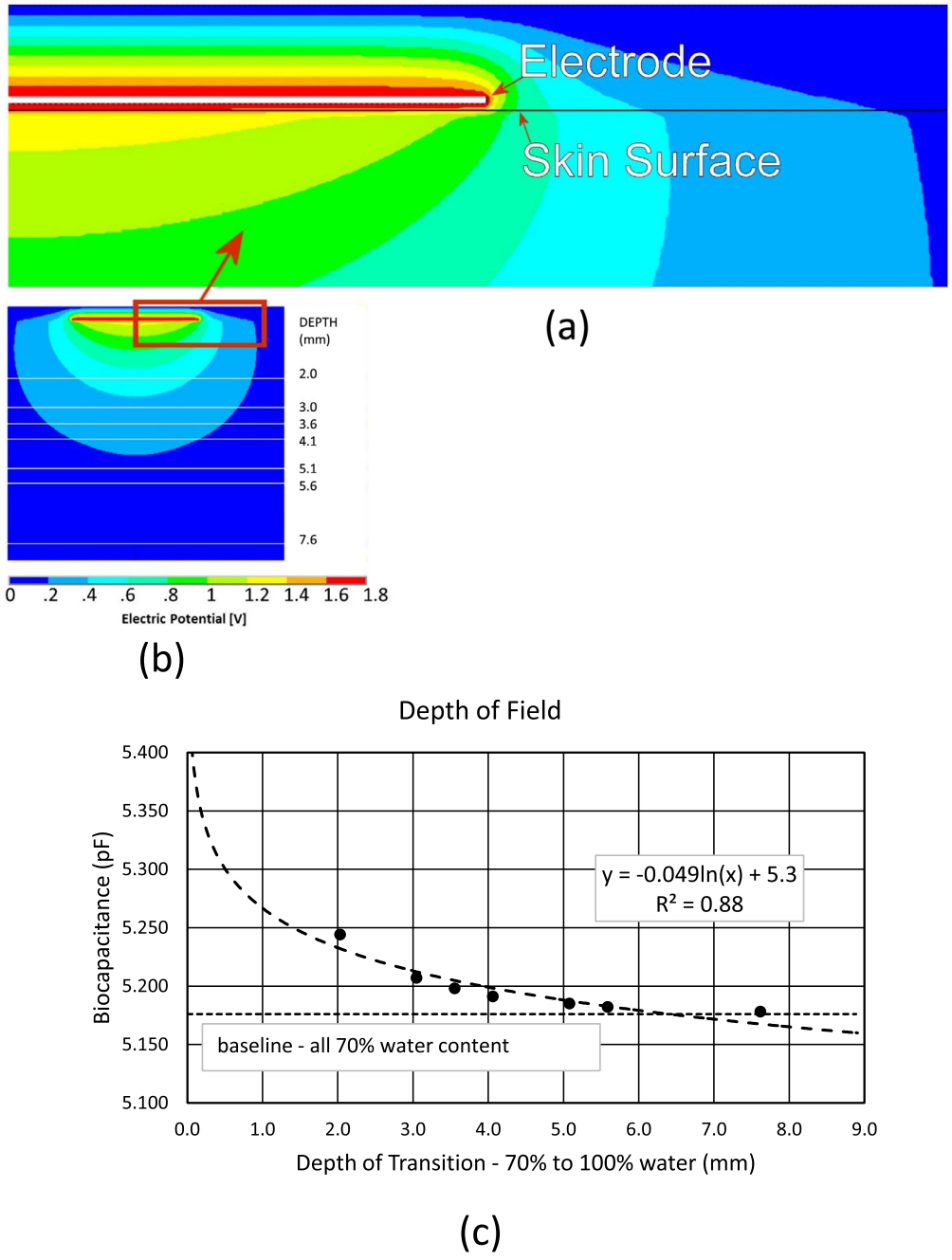

Figure 5. A finite element computational model of the static field generated by the charged SEM sensor is shown (a) as an intensity plot around the center round electrode, the white element inside the red field, shown enlarged in the top figure, and a plot (c) of the calculated biocapacitance detected by the sensor when positioned over the tissue mimic (70% water content) with a deeper layer of pure water at the depth of transition on the *x*-axis, wherein the center of the "knee" in the curve is approximately 3.8 mm.

theoretical upper and lower bounding curves obtained in connection with the aforementioned measurements using the parallel and series model configurations, respectively, are shown in Figure 4c. The red line of Figure 4c is an average of the two bounding models and is a nearly-linear relationship connecting the 0%-water and 100%-water endpoints (plotted as a dashed black line as a guide to the eye).

3.2. Bench test to establish depth of field

The reported SEM values for the various depths of water are shown in Figure 4e. The SEM values increase until the entire field is contained within the water of the pool. Further increases in depth add water beyond the penetration depth of the field, and indeed the SEM reading does not change then. The depth of penetration of the SEM field is therefore determined by the "knee" in the curve that, in this case, is ~3.6 mm (Fig. 4e).

3.3. Computational simulations of the SEM sensor field and sensitivity

The sensor field is shown in Figure 5a,b wherein the center electrode is the white area contained within the red region, with an enlarged view of the region proximate to the edge of the center electrode presented in Figure 5a. The distribution of the electric potential in the simulated 2D field is shown in the gradations

of color from red to dark blue as indicated by the scale in both Figure 5a and b. The field penetrates the deepest directly under the center of the sensor. The field extends radially only a short distance past the outer diameter of the center electrode and does not reach the inner diameter of the toroidal electrode.

Model predictions of the effective biocapacitance are depicted in Figure 5c. The dashed horizontal line is the baseline biocapacitance with only healthy tissue containing 70% water (there is no pure water in the model). At a depth of ~7.6 mm, the capacitance has increased by approximately 0.001 pF (a 0.02% change from the baseline) which is numerically negligible and clinically insignificant. However, at shallower tissue depths the biocapacitance increases substantially and nonlinearly. The heavy dashed line is a best-fit curve for the simulation data, plotted as dots, having the form shown in Figure 5c. Specifically, the plot of biocapacitance versus the depth of the transition to pure water shows a 'knee' in the plotted points having a midpoint in the 3–4 mm range, which is consistent with the experimental results for depth of field (Fig. 4e). Comparing the results of the plot of Figure 5b, wherein the limit of the 0.2 V field potential extends to a depth of ~4.6 mm and the 0.4 V field potential penetrates to a depth of ~2.8 mm, to the curve of Figure 5c, suggests that the limit of detecting an increase of water contents in tissue from 70% to 100% is a field potential of 0.3 V that is consistent with the design of the SEM hardware.

4. Discussion

The noninvasive SEM Scanner technology described here, for assessing the fluid contents of human skin and subdermal tissues to a depth of several millimeters, is novel, clinically effective [15–17] and provides the first useful technological means to assess the health status of tissues below the SC in patients who are at-risk for PIs. Dermatologists, vascular and plastic surgeons, geriatricians, tissue viability nurses and other nursing practitioners are a few examples for health care professionals who diagnose and treat PIs and can therefore immediately benefit from using the SEM Scanner.

Fluid contents in healthy tissues and the associated tissue DCs are bounded between specific, relatively narrow ranges, with fatty tissues having somewhat lower DCs than muscular tissue, hence DCs also depend on the anatomical site being measured and the specific tissue composition there [8–11,14]. Inflammatory conditions, either acute or chronic (e.g. diabetes-related inflammation) are known to alter tissue DCs, and so is lymphedema [1,2]. Changes in the DC have been proposed as a potential biophysical marker for early detection of lymphedema – given the relation between fluid contents and the development of the disease affecting an entire extremity (leg or arm) [1,2,8,14]. Nevertheless, the SEM Scanner is the first technology ever to target more localized fluid content changes for the early indication of increased risk of PIs.

As with any measurement method, the SEM Scanner has limitations. Specifically, the SEM value reported for a particular measurement is affected by the method of use and the skill of the user. The sensor must be in complete contact with the skin, as an air gap immediately adjacent to the sensor will cause a large reduction in the effective DC within the sensor field. Skin-device contact pressures may also affect measurement, but this has been considered in the design of the SEM hardware as explained above. Measurements should be acquired quickly as an extended amount of time under pressure will force fluid away from the area being evaluated by the SEM Scanner. A recent reliability study by Clendenin and colleagues demonstrated very good inter-operator and inter-device agreement (Pearson product correlation coefficient exceeding 0.80) for SEM measurements taken at the sacrum, sternum and heels of healthy individuals [6].

The SEM Scanner is novel, and its measurements are highly beneficial from a clinical perspective. The systematic comparison of near-simultaneous measurements of locally damaged tissue and nearby healthy tissue enables the elimination of multiple common-mode factors, including system pathophysiological conditions. The overall health status of patient, differences in body habitus, local anatomical features and tissue composition between patients, potential differences between scanners and inter-operator differences in measurement techniques are minimized as confounding factors by the delta calculation process used in the SEM Scanner, as described here.

In conclusion, this paper reported the physical and technological principles of operation of the SEM Scanner using an integrated experimental-computational approach. The present SEM Scanner technology and measurement methodology can potentially be applied to identify increased risk for other conditions, for example the tissue damage that precedes a diabetic foot ulcer, as well as military and civilian injury conditions such as traumatic rhabdomyolysis [18]. Such applications would benefit from an ability to scan a larger area with a single device, which could be accomplished using an array of sensors mounted on a flexible substrate, and an ability to monitor a specific body region over time without repeated manual measurements.

Acknowledgments

The work was supported by an unrestricted educational grant from Bruin Biometrics Inc., Los Angeles, CA, USA.

Competing interests

GR is an employee of Bruin Biometrics LLC (BBI) and holds equity in the company. AG is consulting to BBI from which he received support for his research in pressure ulcer prevention. These relationships had no influence on the study design, conduct, analysis of data and interpretation of the results.

Funding

Bruin Biometrics LLC (BBI).

Ethical approval

Not required.

References

[1] Bates-Jensen BM, McCreath HE, Nakagami G, Patlan A. Subepidermal moisture detection of heel pressure injury: the pressure ulcer detection (PUD) study outcomes. Int Wound J 2018;15(2):297–309.
[2] Bates-Jensen BM, McCreath HE, Patlan A. Subepidermal moisture detection of pressure induced tissue damage on the trunk: the pressure ulcer detection (PUD) study outcomes. Wound Repair Region 2017;25(3):502–11.
[3] Bates-Jensen BM, McCreath HE, Pongquan V, Apeles NC. Subepidermal moisture differentiates erythema and stage I pressure ulcers in nursing home residents. Wound Repair Regen 2008;16(2):189–97.
[4] Bishop O. Electronics – a first course. 2nd ed. Elsevier; 2002.
[5] Chen T, Song J, Bowler JR, Bowler N. Analysis of a concentric coplanar capacitive sensor using a spectral domain approach. In: Proceedings of American Institute of Physics (AIP) conference; 2011. p. 1335. doi:10.1063/1.3592126.
[6] Clendenin M, Jaradeh K, Shamirian A, Rhodes SL. Inter-operator and inter-device agreement and reliability of the SEM scanner. J Tissue Viability 2015;24(1):17–23.
[7] Gefen A. The sub-epidermal moisture scanner: the principles of pressure injury prevention using novel early detection technology. Wounds Int 2018;9(3):10–15.
[8] Gefen A. Managing inflammation by means of polymeric membrane dressings in pressure ulcer prevention. Wounds Int 2018;9:22–8.
[9] Gefen A, Gershon S. An observational, prospective cohort pilot study to compare the use of subepidermal moisture measurements versus ultrasound and visual skin assessments for early detection of pressure injury. Ostomy Wound Manag 2018;64(9):12–27.

[10] Goncharenko AV, Lozovski VZ, Venger EF. Lichtenecker's equation: applicability and limitations. Opt Commun 2000;174:19–32.
[11] Mayrovitz HN. Assessing free and bound water in skin at 300MHz using tissue dielectric constant measurements with the moisturemeterD. Lymphedema. Greene A, Slavin S, Brorson H, editors. Springer; 2015.
[12] O'Dowd J, Callanan A, Banarie G, Company-Bosch E. Capacitive sensor interfacing using sigma-delta techniques. IEEE Sens 2005(Oct–Nov):951–4.
[13] Schreier R, Temes G. Understanding delta-sigma data converters. USA: IEEE Press and Johan Wiley & Sons; 2005.
[14] Schwan H, Kay CF. Capacitive properties of body tissues. Circ Res 1957;5:439–43.
[15] Stewart IJ, Faulk TI, Sosnov JA, Clemens MS, Elterman J, Ross JD, Howard JT, Fang R, Zonies DH, Chung KK. Rhabdomyolysis among critically ill combat casualties: associations with acute kidney injury and mortality. J Trauma Acute Care Surg 2016;80(3):492–8.
[16] Tomaselli P, Shamos MH. Electrical properties of hydrated collagen. I. Dielectric properties. Biopolymers 1973;12(2):353–66.
[17] Wang FT. Biomedical system for monitoring pressure ulcer development Ph.D. thesis. University of California Los Angeles (UCLA) School of Electrical Engineering; 2013.
[18] Warner R, Myers M, Taylor D. Electron probe analysis of human skin: determination of water concentration profile. J Investig Dermatol 1988;90:218–24.